Bioorganic Chemistry 88 (2019) 102913

Contents lists available at ScienceDirect

Bioorganic Chemistry

journal homepage: www.elsevier.com/locate/bioorg

In-silico design and synthesis of N9-substituted β-Carbolines as *PLK-1* inhibitors and their *in-vitro/in-vivo* tumor suppressing evaluation

Gomathi Priya Jeyapal[a], Rajendiran Krishnasamy[b], Carolyn K. Suzuki[c], Sundararajan Venkatesh[c], M.J.N. Chandrasekar[a,*]

[a] Department of Pharmaceutical Chemistry, JSS College of Pharmacy (JSS Academy of Higher Education & Research, Mysuru), Ootacamund 643001, Tamil Nadu, India
[b] Department of Pharmacognosy and Phytochemistry, JSS College of Pharmacy (JSS Academy of Higher Education & Research, Mysuru), Ootacamund, Tamil Nadu, India
[c] Department of Microbiology, Biochemistry & Molecular Genetics, New Jersey Medical School-Rutgers, The State University of New Jersey, Newark, NJ, USA

ARTICLE INFO

Keywords:
β-Carboline
PLK-1
Anticancer
Cytotoxicity
Apoptosis
Cell cycle

ABSTRACT

A new series of β-Carboline/Schiff bases was designed, synthesized, characterised and biologically evaluated as inhibitors of *PLK-1*. The synthesized compounds exhibited strong to moderate cytotoxic activities against NCI-60 panel cell assay. Compound SB-2 was the most potent, particularly against colon with GI_{50} of 3–45 μM on NCI-60 panel cell lines. SB-2 selectively inhibited *PLK-1* at 15 μM on KinomeScan screening. It also showed a dose-dependent cell cycle arrest at S/G2 phase on HCT-116 and induced apoptosis by the activation of procaspase-3 and cleaved PARP. Further, the antitumor studies on DLA and EAC model revealed that SB-2, at 100 mg/kg/bd.wt significantly increased their average lifespan. Further, a decrease in the body weight of the tumor-bearing mice was also observed when compared to the tumor controlled mice. SB-2 thus shows good potential as antitumor agent.

1. Introduction

Cancer is still one of the leading causes of death worldwide despite advanced diagnostic and treatment options. In recent years, small molecule kinase inhibitors have emerged as potent anticancer agents. Kinases are among the first identified oncogenes and have become one of the most intensively pursued class of anticancer agents [1]. Currently, more than 130 kinase inhibitors are reported to be in Phase-2/3 clinical trials.

Polo-like kinase-1 (*PLK-1*) is a family of serine/threonine protein kinases which are widespread in eukaryotic cells. It is one of the most investigated kinase as it plays multiple roles in the progression of the cell cycle [2]. *PLK-1* is essential for precisely regulating the cell division and maintaining genome stability in mitosis, spindle assembly and DNA damage response [3]. It is also highly expressed in most of the human cancers and its overexpression is associated with poor prognosis of cancer.

The *PLK-1* contains a highly conserved *N*-terminal kinase catalytic domain and a C-terminal polo-box domain which is connected by a hinge region in the middle. The *N*-terminal has a STK domain with a *T*-loop whose phosphorylation is directly related to the activity of *PLK-1* [4]. The X-ray crystal structure of *PLK-1* shows a bulky phenylalanine at the bottom of the binding site combined with a smaller cysteine in the roof of the pocket (valine in many other kinases) which can accommodate a large molecule in the binding pocket. Further, a pocket created by Leu132 in *PLK-1* (earlier predicted not to be present in other isoforms) provides an opportunity for the design of potent and specific *PLK-1* inhibitors [5].

Though investigations carried out so far have focused on the discovery of more effective and specific *PLK-1* inhibitors [6], there is scope for inventing newer and novel inhibitors with even more selectivity and specificity.

β-Carbolines are a group of heterocyclic compounds that possess a common tricyclic pyrido[3,4-*b*]indole ring structure and are reported to have a wide range of biological activity (Fig. 1). During the last decade, considerable interest has been shown by several investigators on this

Abbreviations: PLK-1, Polo Like Kinase; SRB, Sulforhodamine B; DLA, Dalton's lymphoma ascites; EAC, Ehrlich's ascites carcinoma; NCI-60, National Cancer Institute 60 Cell; PARP, poly ADP ribose polymerase; STK, Serine/Threonine kinase; SAR, Structure activity relationship; QSAR, Quantitative structure activity relationship; ADME/T, Absorption, distribution, metabolism, excretion & toxicity; DS4.1, Discovery Studio 4.1; TMS, tetramethylsilane; TLC, thin layer chromatography; PMA, Phosphomolybdic acid; OECD, Organisation for Economic Co-operation and Development; CMC, sodium carboxy methyl cellulose (0.3%); 5-FU, 5-Fluorouracil; ALS, average life span; % ILS, Percentage increase in life span; PSA, Polar surface area; MTD, Maximum tolerated dose

* Corresponding author at: Dept. of Pharmaceutical Chemistry, JSS College of Pharmacy, Ootacamund, 643001 The Nilgiris, Tamil Nadu, India.
E-mail address: ncsekar@jssuni.edu.in (M.J.N. Chandrasekar).

https://doi.org/10.1016/j.bioorg.2019.04.007
Received 13 August 2018; Received in revised form 22 March 2019; Accepted 5 April 2019
Available online 11 April 2019
0045-2068/

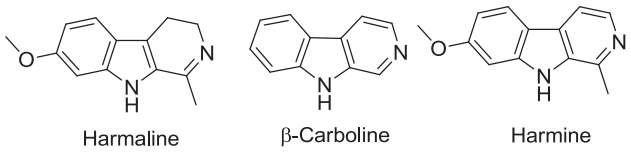

Fig. 1. β-Carboline scaffold and its derivatives.

family of compounds due to their promising antitumor activity through various mechanisms [7–13]. The activity is due to the planarity of the scaffold which can fit into the active site of the numerous protein binding pockets. Modification of β-Carboline scaffold at different positions can, therefore, give lead compounds for different tumor targets. Earlier, it has been observed that substitution at 1, 3 and 9 position of β-Carboline scaffold increases the antitumor potential and decreases the toxicity profile.

Considering the several SAR, QSAR and biological studies carried out so far on β-Carbolines through various target associated mechanisms, these newer and novel carboline derivatives could be a valuable template for antitumor potential. Though a large number of 1,3-substituted β-Carboline derivatives have been reported, a thorough analysis of literature revealed only a very few compounds with heterocyclic and fused ring substitutions at position 9 of β-Carboline, have been synthesized and evaluated for their antitumor potential [14].

In the present study, we report the design, synthesis and evaluation of a series of novel N9 substituted β-Carboline derivatives as *PLK-1* inhibitors for their anticancer potential.

2. Experimental

2.1. Molecular docking and ADME/T studies

In silico molecular docking studies were performed using DS4.1 software. A virtual library was generated based on previous literature and SAR properties of the scaffold [15–17]. The X-ray crystal structure of the *PLK-1* (2OWB) was downloaded from RCSB Protein Data Bank. All the heteroatoms and water molecules were removed from the crystal structure prior to docking and the missing residues were added. All the proteins and ligands were standardized by applying the CHARMm forcefield to the proteins and monitoring the valences of the ligands using Prepare Protein and Prepare Ligand protocols.

The Prepare Protein protocol prepares the *PLK-1* protein by performing tasks such as inserting missing atoms in incomplete residues, modeling missing loop regions, deleting alternate conformations (disorder), removing water molecules, standardizing atoms and protonating titratable residues. The Prepare Ligand protocol helps to prepare ligands for input into other protocols, performing tasks such as removing duplicates, enumerating isomers and tautomers and generating 3D conformations. After the preparation, the active site (binding site) of the protein was first identified and defined based on the ligand already present in the PDB file. A sphere was defined around the binding site for *PLK-1* protein. The binding site sphere is required for running LibDock in Discovery Studio. LibDock uses the systematic conformational search algorithm to dock ligands freely to the receptor and rank the compounds via the default scoring function LibDock Score [18].

The docking protocol was then validated using self-docking analysis of bound crystal ligand back with the same binding pocket. Molecular docking was performed for the designed library of molecules by LibDock protocol. Based on the LibDock score, further simulated annealing docking was performed using CDOCKER protocol in CHARMm based molecular dynamics algorithm with default parameters [19].

CHARMm is a program for molecular simulation and modelling [20]. It uses energy minimization techniques to optimize the conformations, performs molecular dynamics simulation, and analyzes the simulation results to determine structural, equilibrium, and dynamic properties. In order to explore the mode of action of the inhibitor-protein interaction and to highlight the key residues responsible for the binding affinity, interaction energies for each inhibitor were further decomposed into individual residue contributions using the "Calculate Interaction Energy" protocol in Discovery Studio. The CDOCKER interaction energy and interacting residues at active site region were calculated and compared with the bound co-crystal ligand and known inhibitor. The binding energy of protein and ligands were calculated by using the equation:

$$\text{Ebinding} = (Ecomplex) - (Ereceptor + Eligand)$$

The calculated binding energies of standards were used as the baseline comparison for the selection of molecules with the best binding affinity to selected targets. Ligand interactions were analysed for both the originally bound and docked standards with the aid of 2D protein-ligand interaction diagrams. Ligand interactions of the hit molecules were also analyzed to compare the interactions with that of the known inhibitor. The compounds with the best binding affinity were further screened *in silico* for their pharmacokinetics and pharmacodynamics properties using the ADME and Toxicity prediction employing computer-assisted technology (TOPKAT) protocols of DS4.1 [21]. The solubility, absorption, plasma protein binding, CYP2D6 inhibition, and hepatotoxicity of the compounds were evaluated by using ADME/T descriptors. TOPKAT calculations were performed to determine the probability for carcinogenicity, mutagenicity and other toxicity measures of the designed molecules. The molecules which showed good score, binding energy, best conformations and suitable ADME/T profiles were identified as leads and selected for synthesis.

2.2. Chemistry

2.2.1. Chemicals and reagents

The major chemicals used were procured from Sigma and Merck. All other chemicals and reagents used were of analytical grade. The solvents were purified and dried according to standard methods. ^{1}H and ^{13}CNMR spectra were recorded on a Bruker 400 MHz spectrometer using TMS as the internal standard. DMSO-d_6 was used as the solvent. Chemical shifts are reported in parts per million (ppm) downfield from TMS. Spin multiplicities are described as s (singlet), d (doublet), t (triplet), q (quartet), and or m (multiplet). HRMS analysis was recorded on TOF MS ES+ spectrometer. Analytical TLC was performed on MERCK Aluminium back precoated silica gel 60 – F254 (0.5 mm) plates. Visualization of the spots on TLC plates was achieved by exposure to Ninhydrin, PMA, iodine vapor or UV light. Column chromatography was performed using silica gel 60–120 and 100–200 mesh. Moisture sensitive reactions were carried out using standard syringe septum techniques under an inert atmosphere of nitrogen.

2.2.2. General procedure for the synthesis of the key intermediate (Scheme 1)

(I.) Synthesis of ethyl 2-(9H-pyrido[3,4-*b*]indol-9-yl)acetate (NAC):

Norharmane (5 g, 29.8 mM) was dissolved in anhydrous DMF (50 mL) under inert gas and ethyl chloro acetate (1.2 eq.) was added to the solution in the presence of sodium hydride (1.5 eq.) in icecold condition. The mixture was stirred for 24 h at room temperature, quenched with ice cold water and extracted with ethyl acetate. After removal of the solvent under reduced pressure, the resulting residue was purified by silica gel column chromatography using ethyl acetate and *n*-hexane as mobile phase when a pale beige colour compound, NAC, was obtained.

(II.) Synthesis of 2-(9H-pyrido[3,4-*b*]indol-9-yl)acetohydrazide (CAH):

The purified NAC was refluxed with 99% hydrazine hydrate (1 eq.) in ethanol for 24 h. The light yellow colour precipitate formed was filtered and recrystallized in hot ethanol. The hydrazide, CAH, was obtained in good yield.

2.2.3. General procedure for the synthesis of Schiff bases (Scheme 2)

Equal proportions of CAH (1 eq.) and the appropriate aromatic/heterocyclic aldehydes (1 eq.) in dry methanol (20 mL) was boiled under reflux for 12 h in the presence of a few drops of glacial acetic acid. After completion of the reaction, the solvent was removed under reduced pressure. The precipitate was filtered under suction. The resulting residue was washed with excess water and purified by recrystallization using suitable solvents that resulted in compounds, SB-1 to SB-10.

2.3. In vitro cytotoxicity by MTT assay

Vero and PC-3 cell cultures used in the experiments were procured from National Centre for Cell Sciences, Pune, India. Vero and PC-3 cells were grown in Earl's Minimal Essential Medium supplemented with 2 mmol L-glutamine, 10% fetal bovine serum, penicillin (100 µg/mL), streptomycin (100 µg/mL) and amphotericin B (5 µg/mL) and the cells were maintained at 37 °C in a humidified atmosphere with 5% CO_2 and sub cultured twice a week.

The monolayer cell culture was trypsinized and the cell count was adjusted to 10x10^5 cells/ml using DMEM medium containing 10% FBS. To each well of a 96 well microtitre plate, 100 µL of the diluted cell suspension (ca. 10,000 cells/well) was added. After 24 h, when a partial monolayer was formed, the supernatant was flicked off. The monolayer was washed once with the medium. Different test sample concentrations (100 µL) prepared in maintenance media were added per well to the partial monolayer in microtitre plates. The plates were then incubated at 37 °C for 72 h in 5% CO_2 atmosphere. The observations recorded every 24 h. The sample solutions in the wells were discarded after 72 h and 20 µL of MTT (2 mg/mL) in MEM-PR (MEM without phenol red) was added to each well. The plates were shaken gently and incubated for 3 h at 37 °C in 5% CO_2 atmosphere. The supernatant was removed and 50 µL of isopropanol was added. The plates were shaken gently to solubilize the formed formazan. The absorbance was measured at 540 nm on a microplate reader. Using the following formula, the percentage growth inhibition was calculated and the concentration of the drug/test samples needed to inhibit cell growth by 50%, were generated from the dose–response curves for each cell line.

$$\%\text{Growth viability} = \left(\frac{\text{Mean OD of the individual test group}}{\text{Mean OD of the control group}}\right) \times 100$$

2.4. Cytotoxicity screening

The compounds were screened for their cytotoxicity at the Developmental Therapeutics Program, National Cancer Institute, Rockville, Maryland, USA, in their NCI 60 Cell panel screen, initially at a single high dose (10^{-5}M) according to the standard procedure mentioned in the website https://dtp.cancer.gov/discovery_development/nci-60/methodology.htm. The compounds that satisfied predetermined threshold inhibition criteria in a minimum number of cell lines were taken to the full 5-dose assay.

2.5. In vitro short term toxicity studies

The short term toxicity studies were carried out against DLA and EAC cells using standard procedures. This test relies on the breakdown of membrane integrity determined by the uptake of a dye (Tryphan blue) to which the cell is normally impermeable. Cells were cultured in peritoneal cavity of mice by injecting intraperitoneally a suspension of cells (1×10^5 cells/mL). The peritoneal fluid containing cells were withdrawn from the peritoneal cavity between 12 and 15 days with the help of a sterile syringe. The cells were washed with HBSS and centrifuged for 10–15 min at 1200 rpm. The procedure was repeated thrice. The cells were suspended in a known quantity of HBSS and the cell count was adjusted to 1x10^5 cells/mL. The diluted cell suspension was distributed into Eppendorf tubes (0.1 mL containing 2×10^5 cells). The cells were exposed to test dilutions and incubated at 37 °C for 3 h. After 3 h, equal quantities of the treated cells and Tryphan blue (0.4%), were mixed and left for a min and loaded into a haemocytometer and the viable and non-viable count were recorded within two min. (If kept longer, live cells also generate and take up colour). Viable cells do not take up colour, whereas dead cells take up colour. The percentage growth inhibition was calculated and CTC_{50} value was generated from the dose-response curves for each cell line.

$$\%\text{Growth Inhibition} = 100 - \left(\frac{\text{Total cells} - \text{Dead cells}}{\text{Total cells}}\right) \times 100$$

2.6. KINOME scan screening

The KINOME scan screening platform employs a novel and proprietary active site-directed competition binding assay to quantitatively measure interactions between test compound and more than 450 human kinases and disease relevant mutant variants. The kinase profiling study was performed at DiscoverX, USA KINOME*scan*™ Profiling service, using their standard protocol mentioned in the website https://www.discoverx.com/technologies-platforms/competitive-binding-technology/kinomescan-technology-platform/kinomescan-assay-process on selected 25 kinases for the test compound SB-2 at 15 µM.

2.7. Cell cycle analysis

HCT-116, colon carcinoma cells were grown in 60 mm plate at 40% confluence in complete growth medium and treated with SB-2 at a concentration of 0, 5, 10 and 20 µM for 48 or 75 h. At the end of the treatment, cells were trypsinized, harvested and washed once with PBS by centrifuging at 2000 rpm for 5 min at room temperature. The cells were then suspended in the propidium iodide hypotonic solution (0.025gm PI + 0.5 gm sodium citrate + 500 mL ddH_2O, refrigerated and protected from light) and vortexed vigorously to avoid doublet or clumping of cells. The suspension was stored on ice for at least 15 min before running on the flow cytometer. The nuclei suspension should remain on ice until the run. Flow cytometer (Becton Dickinson FACS scan) set up with a blue laser (488 nm) and detection filter (610/20 nm) bandpass for PI was used. Cell flow rate (less than 400 events/*sec*) for optimal resolution of PI fluorescence was set up and doublets were excluded by creating a combination of same-channel bivariate plots utilizing Area vs Height or Area vs Width (*i.e.,* FSC, SSC and PI fluorescence). Singlet events are presented in a diagonal pattern as doublets/clumps have a lower height and higher width values. Fluorescence was acquired and the cell cycle stages were analyzed of each sample by flow cytometry Cell-Quest software (Becton Dickinson, Franklin Lakes, NJ).

2.8. Western blot analysis

Colon carcinoma cell line (HCT) were cultured in DMEM with 10% FBS. The cells were grown in 5% CO2 at 37 °C. On the previous day of the treatment, cells were split into 6 well plates at a confluence of 60–70% overnight. The following day, compound, SB-2 in DMSO was diluted in complete growth medium at a concentration of 20, 10, 5, 2.5, 1.25, 0 µM and replaced in the 6 well plate. SB-2 treated HCT cells were grown for 24 or 48 h. At the end of the treatment, the cells were harvested by using trypsin by centrifuging at 14000 rpm, 4 °C and washed twice with ice-cold PBS and stored at −80 °C until further analysis. Proteins from the cell pellet were extracted by adding the Triton lysis buffer [Triton X-100 buffer (50 mM Tris), (pH 7.5), 300 mM NaCl, and 0.5% Triton X-100] containing 2X phosphatase and protease inhibitor (Thermo Scientific) for 20 min on ice. After centrifugation at 14000 rpm for 15 min at 4 °C, the supernatant was collected and estimated for

protein concentration by the Bradford's method. The protein (40-50μg) was separated by 12% SDS-PAGE, transferred on to the nitrocellulose membrane (100 V, for 72 min) and immunoblotted with respective primary and HRP-conjugated secondary antibodies. Immunoblots were developed by chemiluminescence.

2.9. In vivo screening

Out of the 10 molecules synthesised, SB-2, showed potent activity in both *in silico* and *in vitro* cytotoxicity studies. The compound also proved effective in short term *in vitro* cytotoxicity studies. The compound was, therefore, selected for *in vivo* anticancer activity in different tumor models. The experimental protocols were approved by the Institutional Animal Ethical Committee on animal experimentation of JSS College of Pharmacy, Ootacamund, Tamilnadu, India, [JSSCP/IAEC/PhD/Ph.Chem/02/2016–17].

2.9.1. Acute oral toxicity studies

The compound, SB-2, was evaluated for acute oral toxicity in female Swiss albino mice as per OECD guideline for testing of chemicals, "Acute oral toxicity study (acute toxic class method), Guideline No 423". A limit test at a dose of 2000 mg/kg/bd.wt. was carried out with six female mice. Overnight fasted mice (16–18 h) were weighed and the prepared test substance was administered in a single dose (2000 mg/kg) by oral gavage at a dose of 10 mL/kg/bd.wt. Animals were observed individually after dosing at 0, 30 min and there after an hourly basis with special attention given during the first 4 h and periodically during the first 24 h and daily thereafter for a total of 14 days. Individual weights of animals were recorded on day-0 (non-fasting), day-1 (fasting) shortly before the test substance was administered, on day 7 and 14. Weight changes were calculated and recorded.

2.9.2. In vivo anticancer studies

(I) Selection and maintenance of animals required for anticancer studies

Adult male Swiss albino mice (25–30 g) were used for the study. They were housed in a groups of 6 per cage at 22 ± 1 °C for 12 h light/12 h dark cycle. All the animals were acclimatized to the laboratory environment for at least 48 h before the experiments. Food and water were allowed ad libitum.

(II) Preparation of test compound and standard

The compound, SB-2, was suspended in distilled water using 0.3% CMC and 5-FU was used as the standard.

(III) Effect of SB-2 on mice bearing DLA cells

DLA cells were procured from Amala Cancer Institute, Amala nagar, Trissur, Kerala, India. The cells were maintained *in vivo* in Swiss albino mice intraperitoneally. Swiss albino mice were divided into five groups with six animals in each group. All the animals were injected with DLA cells (1×10^5 cells) intraperitoneally except the normal control group. This was taken as day zero. Group I served as normal control and Group II as tumor control. These two groups received CMC suspension (0.3%) administered orally. Group III served as a positive control and was treated with standard 5-FU at 20 mg/kg p.o. Group IV and V were treated with SB-2 at a dose of 50 and 100 mg/kg p.o., respectively. All these treatments were given 24 h after the DLA cells were inoculated, once daily for 10 days.

(IV) Effect of SB-2 on mice bearing EAC cells

Ehrlich tumor is a rapidly growing carcinoma with very aggressive behavior. It grows in almost all mice strains. The Ehrlich ascitic tumor, derived from a spontaneous murine mammary adenocarcinoma, is maintained in the ascitic form by passaging in Swiss albino mice, by intraperitoneal route. The protocol for this study was the same as described earlier for the DLA model. The following antitumor parameters were calculated for both DLA and EAC experimental models;

Average life span

Life span of the animals of all the groups was noted and the average life span (ALS) was calculated for each group.

$$ALS = \frac{\sum survival\ \ time\ \ [days]\ \ of\ \ each\ \ mice\ \ in\ \ a\ \ group}{Total\ \ number\ \ of\ \ mice\ \ in\ \ a\ \ group}$$

The Kaplan Meier survival curve was plotted for all the groups. Percentage increase in life span (% ILS) was calculated from the average life span.

$$\%ILS = \frac{ALS\ \ of\ \ treated\ \ group - ALS\ \ of\ \ Control\ \ group}{ALS\ \ of\ \ Control\ \ group} \times 100$$

Body weight analysis

Body weight of the experimental mice were recorded for both the treated and control groups, at the beginning of the experiment (day 0) and sequentially on every alternate days during the treatment period. Increase in body weight was observed using statistical analysis. All values are expressed as mean ± SD. Statistical calculation was performed by One-way Analysis of Variance (ANOVA) followed by Tukey's multiple comparison test. The results were considered statistically significant if $P < 0.05$.

3. Results and discussion

3.1. Designing of novel β-Carboline based ligands

A virtual library of 750 β-Carboline analogs, substituted at the N9 position with different heterocycles such as 1,3,4-oxadiazole, 1,2,4-triazole, 1,3,4-thiadiazole, pyrrole, thiophene, imidazole, furan, and a fused ring, naphthalene, was designed. The molecules were substituted with different aldehydes and heterocycles at the amino group of 1,3,4-oxadiazole, 1,2,4-triazole, and 1,3,4-thiadiazole. Additionally, a series of Schiff bases were designed by substituting the N9 position of β-Carboline with five, six-membered and fused rings. A series of 1,3,4-oxadiazole thione derivatives were also designed using different amines and aldehydes. All the designed molecules were identified as novel compounds by SciFinder.

3.2. Molecular docking & ADME/T study

Molecular docking study is the basis for analyzing selectivity and further improvement of a ligand for specific inhibitor development. The docking protocol used was validated by docking the co-crystallized ligand into the X-ray crystal structure of *PLK-1* (2OWB). The superimpositions indicated that the docked complex and crystal conformation overlapped well with the acceptable rms deviation of 0.5 Å which is within the permissible range, as a value of below 2.0 Å is considered being a successful docking protocol. The ligands produced a large number of conformations in the Prepare Ligand protocol. All the conformations were docked against the target protein *PLK-1*. Unique features of the *PLK-1* ATP binding site provide an opportunities for designing of potent and selective inhibitors [5].

Among the 750 molecules designed with various heterocycles, the molecules substituted with Schiff bases at the 9th position of the β-Carboline resulted in good docking scores for the target *PLK-1* compared with the known inhibitor, BI-2536 and the co-crystal ligand

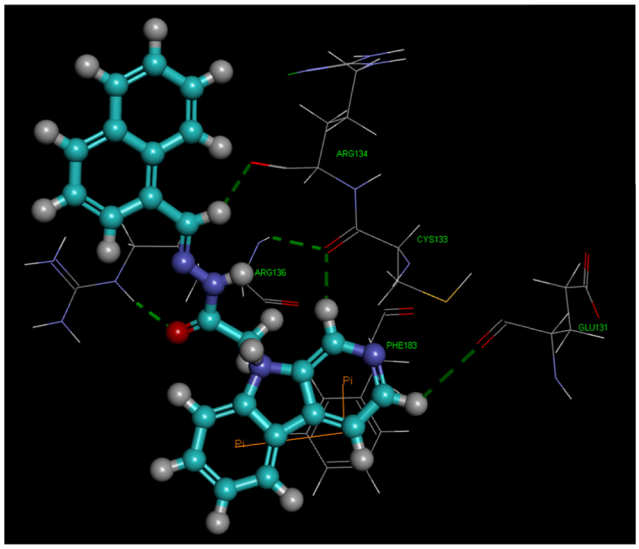

Fig. 2. Molecular interactions of compound SB-2 with *PLK-1* (Dotted green lines represent the H-bond interaction). (For interpretation of the references to colour in this figure legend, the reader is referred to the web version of this article.)

(Table S1). This specificity is due to the presence of C═O linker in the designed molecules and the unique features of the *PLK-1* kinase domain. The designed molecules were well accommodated in the ATP-binding pocket of the *PLK-1* kinase domain. The residues most frequently involved in the interactions were Phe183, Arg136, Cys133, Cys67, and Arg134 (Table S2). The molecules were ranked on the basis of the high docking score, interaction energy, in addition to favorable H-bond, electrostatic and hydrophobic interactions.

Among the best ranked Schiff bases, the molecule, SB-2, substituted with naphthyl ring showed the highest docking score and favorable key interactions with the active site amino acids like the standard *PLK-1* inhibitor, BI-2536 (Fig. S1) and co-crystal (Fig. S2). The C═O group present in the molecule forms a hydrogen bond interaction with the unusual residue, Arg136 which is located in the hinge region of the ATP-binding pocket with a bond distance of 3.2 Å. Another H-bond interaction was found between the key residue of Cys133 in the hinge region of *PLK-1* and –N atom of the pyridyl ring present in the core β-Carboline scaffold with the calculated distance of 3.6 Å (Fig. 2).

The aromatic and pyridyl ring present in the β-Carboline scaffold forms bidentate Pi-Pi interaction with the Phe183. The two aromatic rings of the naphthalene ring form Pi-Pi interactions with Arg136 and Arg57. The compound, SB-2, also showed hydrophobic interactions with Val144, Leu130, Leu132, Ala80, Cys67, Lys61, Gly62, Gly60, and Arg134. These multiple interactions collectively contribute to SB-2 binding affinity and specificity for *PLK-1*.

The first 10 ranked molecules which showed good docking scores were further screened for their ADME/T properties using DS4.1 software. The pharmacokinetic parameters of the selected molecules were assessed by biplot ADME descriptions of DS4.1. A plot between AlogP and PSA descriptors at 95% and 99% confidence ellipses was considered to be a more precise model for the cell permeability prediction. The intestinal absorption model includes 95% and 99% confidence ellipses in the ADMET_PSA_2D Vs ADMET_AlogP98 plane, represents the oral absorption of the selected molecules (Fig. S3). The *in silico* oral absorption of the molecules was found to be extremely good and showed good Blood-Brain Barrier penetration. All the molecules had the AlogP < 5 and Polar Surface Area < 140 (PSA), values within the permissible range (AlogP98 –1 to 5.9 and PSA of 0 to 132 $Å^2$). The molecules were found to be non-inhibitors of CYP2D6 enzyme and showed low to moderate solubility (Table S3).

The *in silico* toxicity profile was assessed by TOPKAT model in DS4.1. The molecules did not show any AMES mutagenicity, carcinogenicity and hepatotoxicity. However, some molecules showed mild skin irritancy during *in silico* prediction. In conclusion, all the 10 molecules had good binding interactions and acceptable ADME/T properties. These 10 molecules were, therefore, selected for synthesis.

3.3. Synthesis and characterization of lead molecules

Norharmane was esterified at the N9 position by treating with ethyl chloroacetate in the presence of NaH exhaustively in dry condition to obtain NAC (Scheme 1). NAC was purified by column chromatography and characterized by IR, ^1H, ^{13}C NMR and HRMS analysis. The formation of the ester function was confirmed by the disappearance of –NH peak in IR and ^{1}HNMR. It was also confirmed by the presence of new signals at δ 5.091 (S, N-CH_2), 1.2 (t, terminal $-CH_3$ and 4.2 (q, $-CH_2$ group) ppm, in ^{1}HNMR. The signals at 1195 (C—O), 1733 (C═O), 1442.54 (C—N) and 1626 (C═N) in IR spectra clearly indicate the completion of the reaction. The signal at δ 167.886 ppm in ^{13}CNMR corresponds to the C═O group. The High-Resolution Mass spectrum value matched with the molecular formula and calculated mass of the synthesized compound.

The N9 substituted ester was transformed to hydrazide (CAH) by treating the ester with hydrazine hydrate in ethanol. The formation of the hydrazide was confirmed by the presence of $-NH_2$ peak in IR and ^{1}HNMR. Further, the disappearance of peaks which corresponds to the ester function indicated the conversion of ester to hydrazide. It was also confirmed by the presence of new signals at δ 5.108 (S, N$-CH_2$), 7.3 (t, $-$NH) and 2.5 (d, $-NH_2$ group) ppm, in ^{1}HNMR. The signals at 1649.12 (C═O) and 1442.95 (C—N) in IR spectra clearly indicate the completion of the reaction. The signal at δ 166.90 ppm in ^{13}CNMR corresponds to

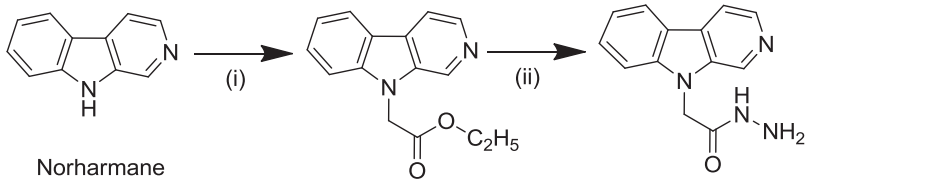

Norharmane
(Beta carboline)

ethyl 2-(9*H*-pyrido[3,4-*b*]indol-9-yl) acetate
(NAC)

2-(9*H*-pyrido[3,4-*b*]indol-9-yl) acetohydrazide
(CAH)

Reaction Conditions:
(i) $ClCH_2COOC_2H_5$, NaH in dry DMF stirred at 0°C to RT for overnight;
(ii) NH_2-NH_2 (99%) in Ethanol at 70°C refluxed for 24h;

Scheme 1. Synthesis of the key intermediate.

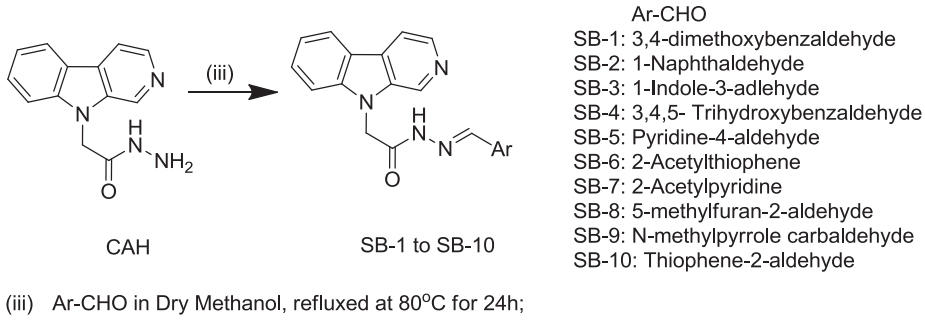

Scheme 2. Synthesis of Schiff bases.

the C═O group present in the amide function.

In Scheme 2, the compounds, SB-1 to SB-10 were prepared by Schiff reaction utilizing hydrazide function and the respective aromatic/heterocyclic aldehydes in good yields. The transformation of the azomethine group by the condensation of respective aldehydes and amine was characterized by the presence of C═N group in IR, ^{1}H, and ^{13}C NMR analysis.

3.4. In vitro cytotoxicity screening by MTT assay

The compounds synthesized through Scheme 2 were evaluated for their preliminary cytotoxicity screening on Vero and PC-3 prostate cancer cell lines by MTT assay. The IC_{50} values were found to be greater than 1 μM against Vero cell lines and 0.1–1.3 μM against PC-3 cell lines (Table S4).

3.5. In vitro tumor cell line screening

In silico docking studies predicted that the designed molecules can bind to *PLK-1* which is up-regulated in multiple cancers including lymphoma, leukemia, multiple myeloma, colon, prostate, gastric, breast, head and neck cancers. A total of 9 compounds were further evaluated for their cytotoxicity against 60 different human cancer cell lines.

All the compounds were initially tested at a single dose at a high concentration (10 μM) in the sixty-cell line panel (One-dose screen). The compounds that satisfied predetermined threshold inhibition criteria in a minimum number of cell lines were taken up for the five-dose assay. The results are presented as the % growth of treated cells relative to the control following 48 h of incubation.

All the compounds showed inhibitory activity ($> = 20\%$) on leukemia HL-60 (TB) cell lines. Among the nine compounds, two compounds, SB-2 and SB-3, showed significant cytotoxic activity against most of the tested human cancer cell lines in the preliminary test. However, SB-2, showed < 20% growth in 25 cell lines and lethality was found in 9 cell lines at 10 μM across the 60-panel cell lines. The results of the one dose screen were summarized in Fig. S4. The compound, SB-3, showed < 50% growth in 23 cell lines and lethality was found with ovarian cancer cell line [OVCAR-4: −60.03] and leukemia cell line [RPMI-8226: −27.72] at 10 μM.

Based on the threshold inhibition criteria, SB-2 was further screened for the five-dose (0.01, 0.1, 1.0, 10 and 100 μM) assay. The compound showed a GI_{50} value in the range of 3–40 μM (Figs. S5 & S6) and exhibited significant cytotoxicity on HCT-116, SR and RPMI-8226 cell lines with GI_{50} values of 3.5, 6.3 and 7.8 μM, respectively.

3.6. Kinase selectivity evaluation

As the molecules were designed towards *PLK-1* inhibition, the inhibitory potential of SB-2 was carried on 25 kinases (Fig. S7) of the STK family. The kinases were selected on the basis of their previous reports available for carboline derivatives. The compound, at a dose level of 15 μM, showed substantial *PLK-1* inhibition (6.2 %control), and a modest inhibition was found with *PIM-2* and *DAPK-3* (Fig. S8), namely 73 and 77 %control, respectively. These results were in tandem with the *in silico* docking results.

3.7. Cell cycle analysis

To elucidate the mechanism by which SB-2 inhibits cell proliferation, its effect on cell cycle was evaluated. HCT-116 cells were treated with 0–20 μM of SB-2 for 48 and 75 h (Fig. 3a & b). The DNA content was analyzed by staining the cells with propidium iodide. The analysis revealed an increase in the percentage of cells in the S phase from 20.16% (untreated control) to 38.29% (20 μM), followed with a concomitant decrease in the percentage of cells in G2 phase. No major change was observed in the percentage of cells in G1 phase exposed at 5 and 10 μM. Only a slight reduction in the percentage of cells was observed in G1 phase at 20 μM after 75 h treatment. After 48 h treatment, an increase in the percentage of cells in S phase was observed from 18.08% (untreated cells) to 36.29% (20 μM of SB-2). Accumulation of cells in G2 phase decreased from 8.0% (untreated) to 3.95% at 20 μM. No major changes in SubG1 peak were observed after 48 and 75 h treatment. These data suggest that, SB-2, induces slight apoptosis and causes the cell cycle arrest between S and G2 phase in HCT-116 cells. It is well known that *PLK-1* expression is activated and peaks at late G2/early prophase. However, its expression starts in DNA replication stage basal level activity [22]. It can be proposed that the S/G2 phase cell cycle arrest by SB-2 in HCT-116 cells may be due to the degradation of *PLK-1* expression.

3.8. Western blot analysis

The induction of apoptotic proteins, procaspase-3 and cleaved PARP, were analyzed by western blot. A dose-dependent upregulation of these protein levels was observed after 48 h treatment indicating that SB-2 induces apoptosis after 48 h. The induction of apoptosis is seen at 2.5 μM with upregulation of caspase 3 at 2.5 μM followed by the cleavage of PARP (Fig. 4). However, treatment after 24 h did not activate these proteins suggesting that SB-2 may be a slow binding inhibitor.

3.9. In vitro short term toxicity studies

In vitro short term toxicity studies were carried out against DLA and EAC cells using standard procedures. The compound, SB-2 was screened at 0–1000 μg/mL concentration on EAC and DLA cell lines. 100% cell death was observed up to 125 μg against EAC and DLA cell lines. The CTC_{50} value of SB-2 was found to be 58 and 65 μg against DLA and EAC cells, respectively.

3.10. Acute oral toxicity studies

Acute oral toxicity was performed on Swiss albino female mice as per OECD guidelines 423. SB-2 at a maximum dose of 2000 mg/kg/bd.wt was

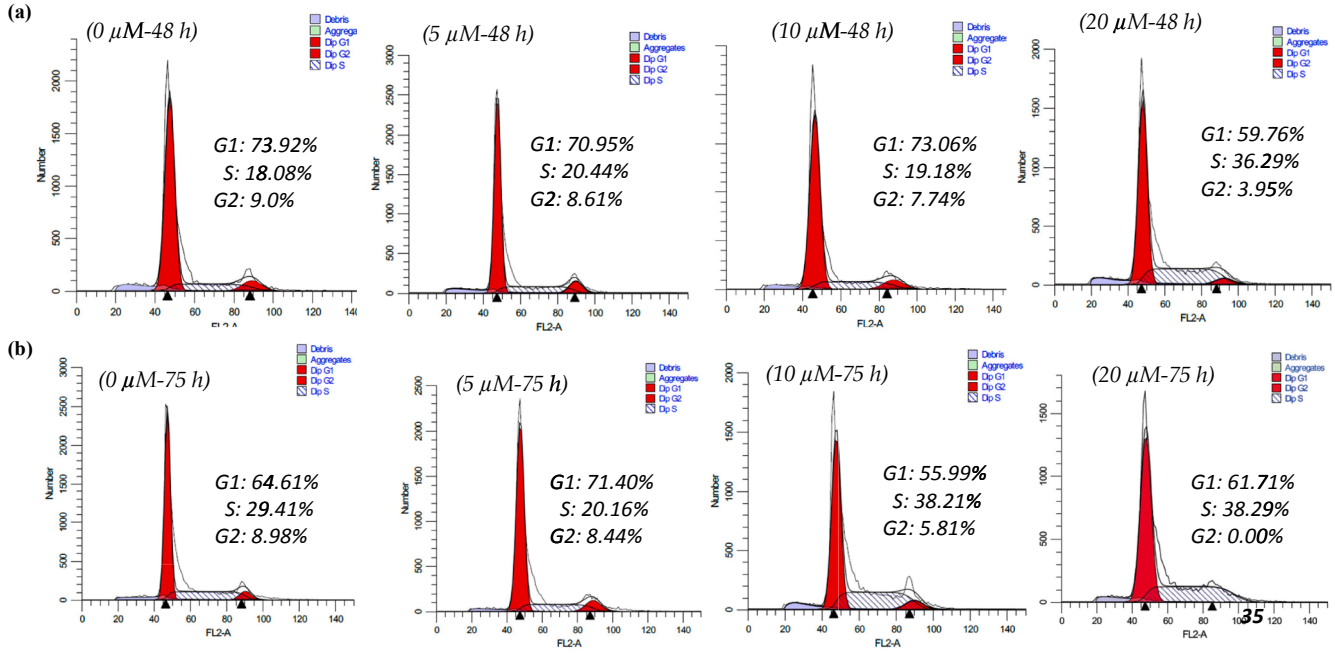

Fig. 3. SB-2 mediated cell cycle arrest in HCT-116 cells after 48 (a) and 75 h (b).

administered at once by the oral route. The mice were observed for a period of 14 days. The compound did not show any toxic signs, abnormal neuronal behaviors and preterminal deaths. All the mice gained weight throughout the observation period. Based on the results, the maximum tolerated dose of the acute oral toxicity of the test compound, SB-2, in Swiss albino mice was fixed as MTD > 2000 mg/kg.

3.11. *In vivo* anticancer studies

As SB-2 showed well *in vitro* cytotoxic potential on selected cancer cell lines, it was further evaluated for *in vivo* anticancer activity on DLA and EAC induced ascites tumor models. Ascitic tumor implantation is known to induce *per se* local inflammatory reactions with an increase in vascular permeability, resulting in an intense edema formation, cellular migration, and a progressive ascitic fluid formation. The ascitic fluid is essential for tumor growth since it constitutes the direct nutritional source for tumor cells [23].

Effect of SB-2 on DLA bearing mice

SB-2 significantly increased the lifespan (Fig. 5) of the tumor induced animals with a significant reduction in the body weight when compared to tumor control mice indicating its potent anticancer properties. The standard, 5-FU at 20 mg/kg, significantly ($p < 0.05$) increased the ALS to 21.33 ± 1.54 days with the % ILS of 45.49%. Treatment with SB-2 at 100 mg/kg significantly ($p < 0.05$) increased the ALS of DLA bearing mice from 14.66 ± 0.66 to 19.66 ± 1.51 days when compared to the DLA tumor control group. Percentage ILS of SB-2 at 100 mg/kg was found to be 34.09% which is comparable to standard 5-FU at 20 mg/kg. Only 11.39% of ILS was observed with 50 mg/kg SB-2 treated group (Table S5).

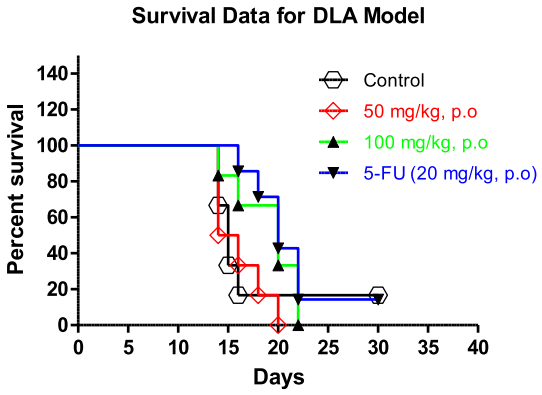

Fig. 5. Kaplan-Meier survival curve for DLA Model.

The change in body weight of treated animals may be due to the reduction in ascitic fluid volume which in turn may have restricted the tumor progression. The increase in body weight of DLA bearing mice was 41.530 ± 3.991. Treatment with SB-2 at 50 and 100 mg/kg/bd.wt showed a significant reduction in the body weight ($p < 0.05$) when compared to DLA tumor control and comparable with normal and standard groups on day 14 (Table S6).

Effect of SB-2 on EAC bearing mice

The standard 5-FU at 20 mg/kg, significantly ($p < 0.001$) increased the ALS to 25.33 ± 1.02 days with the % ILS of 74.68% (Fig. 6).

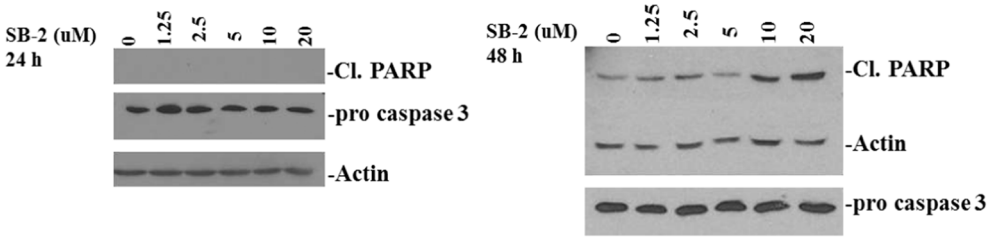

Fig. 4. Western blot analysis of SB-2 in HCT-116 cells after 24 and 48 h.

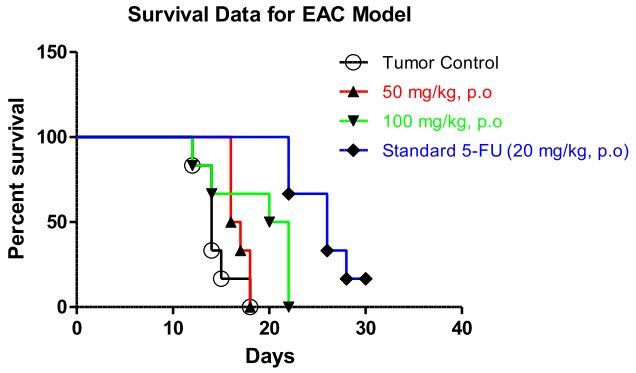

Fig. 6. Kaplan-Meier survival curve for EAC Model.

Treatment with SB-2 at 100 mg/kg significantly ($p < 0.05$) increased the ALS of EAC bearing mice from 14.5 ± 1.09 to 18.66 ± 1.02 days when compared to EAC tumor control group. The lifespan of the animals treated with SB-2 at 50 and 100 mg/kg increased by 28.68 and 16.06%, respectively (Table S7). When compared to the standard, compound, SB-2 showed only a moderate effect on EAC induced model at both the doses tested.

The increase in body weight of EAC bearing mice after 14 days of tumor induction was 41.210 ± 3.991. Treatment with SB-2 at 50 and 100 mg/kg/bd.wt showed a significant reduction in body weight ($p < 0.05$) when compared to EAC tumor control and comparable with normal and standard groups on day 14 (Table S8).

4. Conclusion

A series of novel N9 substituted β-Carboline analogs were designed as potential inhibitors of *PLK-1*. The molecules that showed good binding interactions and acceptable ADME/T properties were synthesized and evaluated for their anticancer activity. It was found that the cytotoxic potential was more pronounced in β-Carboline moiety substituted with a naphthalene ring followed by indole ring. The order of cytotoxic potential was observed as naphthalene > indole > 6-membered heterocyclic > 5-membered heterocyclic rings. The compound, (E)-N'-(naphthalene-1-ylmethylene)-2-(9H-pyrido[3,4-*b*]indol-9-yl) acetohydrazide (SB-2) substituted with a naphthalene ring showed promising caspase-dependent antiproliferative activity. The suppression of cell proliferation may be due to the depletion of *PLK-1* enzyme. The inhibition of *PLK-1* might be due to the interactions between SB-2 and the unusual residues, Arg136 and Leu132, present in the hinge region of *PLK-1* protein. Further studies are in progress to elucidate the mechanism of action for its antiproliferative activity.

Conflict of interest

The authors have no conflicts of interest regarding the content of this article.

Acknowledgement

Author, Gomathi Priya Jeyapal, would like to thank the Department of Science and Technology, Govt. of India, for providing the financial support under Women Scientist Scheme-WOSA (File no: SR/WOS-A/CS-1018/2014). We thank the Developmental Therapeutics Program, National Cancer Institute, USA, for help in screening the cytotoxicity on 60 human tumor cell lines.

Appendix A. Supplementary material

Supplementary data to this article can be found online at https://doi.org/10.1016/j.bioorg.2019.04.007.

References

[1] J. Zhang, P.L. Yang, N.S. Gray, Targeting cancer with small molecule kinase inhibitors, Nat. Rev. Cancer. 9 (2008) 28–39, https://doi.org/10.1038/nrc2559.
[2] Z. Hao, V. Kota, Volasertib for AML: Clinical use and patient consideration, Onco. Targets. Ther. 8 (2015) 1761–1771, https://doi.org/10.2147/OTT.S60762.
[3] C. McInnes, M.D. Wyatt, PLK1 as an oncology target: Current status and future potential, Drug Discov. Today. 16 (2011) 619–625, https://doi.org/10.1016/j.drudis.2011.05.002.
[4] X. Liu, Targeting polo-like kinases: A promising therapeutic approac for cancer treatment, Transl. Oncol. 8 (2015) 185–195, https://doi.org/10.1016/j.tranon.2015.03.010.
[5] M. Kothe, D. Kohls, S. Low, R. Coli, A.C. Cheng, S.L. Jacques, T.L. Johnson, C. Lewis, C. Loh, J. Nonomiya, A.L. Sheils, K.A. Verdries, T.A. Wynn, C. Kuhn, Y.H. Ding, Structure of the catalytic domain of human polo-like kinase 1, Biochemistry. 46 (2007) 5960–5971, https://doi.org/10.1021/bi602474j.
[6] R.E.A. Gutteridge, M.A. Ndiaye, X. Liu, N. Ahmad, Plk1 Inhibitors in Cancer Therapy: From Laboratory to Clinics, Mol. Cancer Ther. 15 (2016) 1427–1435, https://doi.org/10.1158/1535-7163.MCT-15-0897.
[7] L. Mele, M. Massotti, F. Gatta, Neuropharmacology of several b-carboline derivatives and their 9-acetylated esters. In vivo versus in vitro studies in the rabbit, Pharmacol. Biochem. Behav. 30 (1988) 5–11, https://doi.org/10.1016/0091-3057(88)90418-2.
[8] S. Xiao, W. Lin, C. Wang, M. Yang, Synthesis and biological evaluation of DNA targeting flexible side-chain substituted beta-carboline derivatives, Bioorg. Med. Chem. Lett. 11 (2001) 437–441, https://doi.org/10.1016/S0960-894X(00)00679-X.
[9] X. Yu, W. Lin, R. Pang, M. Yang, Design, synthesis and bioactivities of TAR RNA targeting β-carboline derivatives based on Tat-TAR interaction, Eur. J. Med. Chem. 40 (2005) 831–839, https://doi.org/10.1016/j.ejmech.2005.01.012.
[10] Y.H. Wang, J.G. Tang, R.R. Wang, L.M. Yang, Z.J. Dong, L. Du, X. Shen, J.K. Liu, Y.T. Zheng, Flazinamide, a novel β-carboline compound with anti-HIV actions, Biochem. Biophys. Res. Commun. 355 (2007) 1091–1095, https://doi.org/10.1016/j.bbrc.2007.02.081.
[11] P. Gao, N. Tao, Q. Ma, W.X. Fan, C. Ni, H. Wang, Z.H. Qin, DH332, a synthetic β-carboline alkaloid, inhibits B cell lymphoma growth by activation of the caspase family, Asian Pacific J. Cancer Prev. 15 (2014) 3901–3906, https://doi.org/10.7314/APJCP.2014.15.9.3901.
[12] P. Ashok, S. Ganguly, S. Murugesan, Manzamine alkaloids: Isolation, cytotoxicity, antimalarial activity and SAR studies, Drug Discov. Today. 19 (2014) 1781–1791, https://doi.org/10.1016/j.drudis.2014.06.010.
[13] G.P. Jeyapal, R. Krishnasamy, M.J.N. Chandrasekar, J. Selvaraj, In-silico binding approaches of β-carboline derivatives towards the possible antitumor targets, Int. J. Res. Pharm. Sci. 8 (2017).
[14] R. Cao, W. Peng, Z. Wang, A. Xu, B-Carboline Alkaloids: Biochemical and Pharmacological Functions, Curr. Med. Chem. 14 (2007) 479–500, https://doi.org/10.2174/092986707779940998.
[15] J. Zhang, Y. Li, L. Guo, R. Cao, P. Zhao, W. Jiang, Q. Ma, H. Yi, Z. Li, J. Jiang, J. Wu, Y. Wang, S. Si, DH166, a beta-carboline derivative, inhibits the kinase activity of PLK1, Cancer Biol. Ther. 8 (2009) 2374–2383, https://doi.org/10.4161/cbt.8.24.10182.
[16] X. Han, J. Zhang, L. Guo, R. Cao, Y. Li, N. Li, Q. Ma, J. Wu, Y. Wang, S. Si, A Series of Beta-carboline derivatives inhibit the kinase activity of PLKs, PLoS One. 7 (2012) e46546, , https://doi.org/10.1371/journal.pone.0046546.
[17] J.B. Ghasemi, V. Davoudian, 3D-QSAR and docking studies of a series of β -carboline derivatives as antitumor agents of PLK1, J. Chem. 323149 (2014) 10, https://doi.org/10.1155/2014/323149.
[18] S.N. Rao, M.S. Head, A. Kulkarni, J.M. LaLonde, Validation studies of the site-directed docking program LibDock, J. Chem. Inf. Model. 47 (2007) 2159–2171, https://doi.org/10.1021/ci6004299.
[19] G. Wu, D.H. Robertson, C.L. Brooks, M. Vieth, Detailed analysis of grid-based molecular docking: A case study of CDOCKER - A CHARMm-based MD docking algorithm, J. Comput. Chem. '24 (2003) 1549–1562, https://doi.org/10.1002/jcc.10306.
[20] B.R. Brooks, C.L. Brooks, A.D. Mackerell, L. Nilsson, R.J. Petrella, B. Roux, Y. Won, G. Archontis, C. Bartels, S. Boresch, A. Caflisch, L. Caves, Q. Cui, A.R. Dinner, M. Feig, S. Fischer, J. Gao, M. Hodoscek, W. Im, K. Kuczera, T. Lazaridis, J. Ma, V. Ovchinnikov, E. Paci, R.W. Pastor, C.B. Post, J.Z. Pu, M. Schaefer, B. Tidor, R.M. Venable, H.L. Woodcock, X. Wu, W. Yang, D.M. York, M. Karplus, CHARMM: The biomolecular simulation program, n.d. doi:10.1002/jcc.21287.
[21] X. Xia, E.G. Maliski, P. Gallant, D. Rogers, Classification of kinase inhibitors using a Bayesian model, J. Med. Chem. 47 (2004) 4463–4470, https://doi.org/10.1021/jm0303195.
[22] S.-Y. Lee, C. Jang, K.-A. Lee, Polo-like kinases (plks), a key regulator of cell cycle and new potential target for cancer therapy, Dev Reprod. 18 (2014) 65–71, https://doi.org/10.12717/DR.2014.18.1.065.
[23] M. Gupta, U.K. Mazumder, R.S. Kumar, T. Sivakumar, M.L.M. Vamsi, Antitumor activity and antioxidant status of Caesalpinia bonducella against Ehrlich ascites carcinoma in Swiss albino mice, J. Pharmacol. Sci. 94 (2004) 177–184, https://doi.org/10.1254/jphs.94.177.